REPORTS OF PRACTICAL ONCOLOGY AND RADIOTHERAPY 24 (2019) 681–687

Available online at www.sciencedirect.com

ScienceDirect

journal homepage: http://www.elsevier.com/locate/rpor

Original research article

# Biological dose-enhancement analysis with Monte Carlo simulation for Lipiodol for photon beams

*Daisuke Kawahara*[a,*], *Shuichi Ozawa*[a,b], *Hisashi Nakano*[c], *Katsumaro Kubo*[d], *Takehiro Shiinoki*[e], *Tomoki Kimura*[a], *Yasushi Nagata*[a,b]

[a] *Department of Radiation Oncology, Institute of Biomedical & Health Sciences, Hiroshima University, Japan*
[b] *Hiroshima High-Precision Radiotherapy Cancer Center, Japan*
[c] *Department of Radiation Oncology, Niigata University Medical and Dental Hospital, Japan*
[d] *Department of Radiation Oncology, Hiroshima Prefectural Hospital, Japan*
[e] *Department of Radiation Oncology, Graduate School of Medicine, Yamaguchi University, Japan*

ARTICLE INFO

*Article history:*
Received 5 December 2018
Received in revised form
1 August 2019
Accepted 7 October 2019

*Keywords:*
Radiobiological dose enhancement
Lipiodol
Monte Carlo calculation
MK model

ABSTRACT

*Background:* Previously, the physical dose-enhancement factor ($D_{phys}EF$) enhancement was introduced. However, the dose enhancement considering the biological effectiveness was not shown.

*Purpose:* The aim of the current study was to evaluate the biological dose-enhancement factor ($D_{bio}EF$) by the dose rate and to compare the $D_{phys}EF$ and the $D_{bio}EF$ in Lipiodol for liver Stereotactic Body Radiation Therapy (SBRT).

*Materials and methods:* Flattening-filter-free (FFF) 6-MV (6MVX) and 10MVX beams were delivered by TrueBeam. A virtual inhomogeneity phantom and a liver SBRT patient-treatment plan were used. The $D_{phys}EF$ and lineal energy distribution (y) distribution was calculated from Monte Carlo simulations. Using a microdosimetric-kinetic (MK) model that is estimated based on the linear-quadratic formula for Lipiodol using human liver hepatocellular cells (HepG2), the biological dose and biological dose enhancement factor ($D_{bio}EF$) were calculated. The dose rate in the simulation was changed from 0.1 to 24 Gy/min.

*Results:* The $D_{bio}EF$ (DR:2Gy/min) and $D_{phys}EF$ with 10MVX FFF beam were 23.2% and 19.1% at maximum and 12.8% and 11.1% on average in the Lipiodol. In the comparison of the $D_{bio}EF$ between 0.1–24 Gy/min, the $D_{bio}EF$ was 21.2% and 11.1% with 0.1 Gy/min for 6MVX and 10 MVX, respectively. The $D_{bio}EF$ was larger than DEF for the 6MVX and 10MVX FFF beams. In clinical cases with the 10MVX FFF beam, the $D_{bio}EF$ and $D_{phys}EF$ in the Lipiodol region can increase the in-tumor dose by approximately 11% and 10%, respectively, without increasing the dose to normal tissue.

This work was presented at the 59th Annual meeting of the American Association of Physicists in Medicine.

* *Corresponding author at*: Section of Radiation Therapy, Department of Clinical Support, Hiroshima University Hospital, 1-2-3 Kasumi, Minami-ku, Hiroshima 734-8551, Japan.
E-mail address: daika99@hiroshima-u.ac.jp (D. Kawahara).

https://doi.org/10.1016/j.rpor.2019.10.006

*Conclusions:* The lower-energy and higher-dose-rate beams were contributed to the biological dose. The Lipiodol caused the enhancement of the physical dose and biological effectiveness.

*Advances in knowledge:* The biological dose enhancement ($D_{bio}EF$) should be considered in the high-density material such as the Lipiodol.



## 1. Background

Gold Nano-Particle (GNP) is useful for the tumor to be sensitive to damage by dose enhancement.[1] The dose enhancement with GNP can be achieved by using a material of a high atomic number.[2] Recently, radiobiological experiments for dose enhancement were performed with low-energy X-rays.[3,4] Monte Carlo (MC) simulations have been used to analyze the dose enhancement in radiation therapy.[5–8] Our previous study reported the dose enhancement in Lipiodol (Guerbet, Villepinte, France) irradiated by a 10-MV X-ray (10MVX) flattening-filter-free (FFF) beam.[9] Lipiodol, which was used for tumor seeking in trans-arterial chemoembolization, has been used for liver cancer. The removal of the flattening filter decreases beam attenuation and also increases dose enhancement because the FFF beam includes a large number of low-energy photons compared with the flattening-filter (FF) beam.[10]

Although the analysis of the physical dose ($D_{phys}$) enhancement was introduced, the dose enhancement considering the biological effectiveness was not shown. For photon therapy, Joiner et al. reported that damage to the tissue or cells with photon irradiation depends on the photon energy and dose rate.[11] The relative biological effectiveness (RBE) variation with photon energy was observed in the previous studies.[12,13] Our previous study investigated the relative biological effectiveness (RBE) using FF and FFF beams for 6-MV X-ray (6MVX) and 10MVX beams.[14] It revealed that RBE varies owing to the flattening filter and the photon energies. The other study reported that the experiment on the RBE variation was performed for the RBE of killing Human Salivary Gland (HSG) tumor cells irradiated with 6 MVX and 200 kVX beams.[15] However, they could not calculate the dose distribution and only considered the photon energy.

Hawkins et al. developed the microdosimetric kinetic (MK) model which can predict the SF of cells from the physical dose by a domain that is a subcellular structure for any kind of radiation.[16] Inaniwa et al. calculated the biological dose distribution for carbon-ion beams.[17] They showed the difference of the dose distribution due to the effects of delivering a fractioned dose by using the MK model. The dose delivery time depended on the dose rate (DR) and patient re-set up time. Cell killing is decreased with the fraction time because of sublethal damage repair (SLDR).[17] Inaniwa et al. concluded that when the dose delivery time was prolonged to 30 min or more, it was largely influenced in carbon-ion radiotherapy. However, these calculation techniques were not used for photon therapy. Additionally, there is no paper regarding how DR affects dose enhancement.

## 2. Aim

In this study, we calculated the biological dose distribution with and without Lipiodol for 6MVX and 10MVX FFF beams. The biological dose enhancement ($D_{bio}EF$) was evaluated and the effects of the $D_{bio}EF$ due to DR for photon therapy were revealed.

## 3. Methods and materials

### 3.1. *Physical dose calculation with MC*

A TrueBeam linac (Varian Medical Systems, Palo Alto, USA) for FFF beams of 6MVX and 10MVX was modelled. The components of linac's head are proprietary and the direct simulation cannot be performed. Varian provides IAEA-compliant phase-space files that were simulated using the GEANT4 MC code, located just above the secondary X/Y collimator. Therefore, we modelled the phase-space files below the secondary collimator using BEAMnrc, which is an important special-purpose code built on the EGSnrc platform.[18] These phase-space files scored at a source-to-surface distance (SSD) of 70 cm are used as a source in the Particle and Heavy Ion Transport Code System (PHITS) calculation. The dose calculation and biological effect were calculated using PHITS.[19] The historic numbers of the photons were $2.0 \times 10^8$ in BEAMnrc and $2.0 \times 10^9$ in PHITS, respectively. The grid size for the dose-calculation was 2.0 mm. The energy cut-off for electrons and photons were set to 0.7 MeV for electrons kinetic plus rest energy and 0.01 MeV for photons. The validation of MC calculations was performed by comparing them with the measurements. The percent depth dose (PDD) curve was obtained using a CC04 (IBA Dosimetry, TN, USA) chamber for a $10 \times 10\,cm^2$ field.

For the dose calculations, a virtual phantom and clinical patient Computed Tomography (CT) image were created. The virtual inhomogeneity phantom was created with a water-equivalent phantom ($20 \times 20 \times 20\,cm^3$) where Lipiodol ($3 \times 3 \times 3\,cm^3$) was inserted at a depth of 5.0 cm (Fig. 1). The cross-section data and physical density of Lipiodol, each milliliter of which contains 480 mg/mL of Iodine organically combined with the ethyl esters of fatty acids of poppy-seed oil, were assigned on PHITS with EGS incorporated.[20] The Lipiodol has a physical density of $1.28\,g/cm^3$. The field size of the beam was set to $5 \times 5\,cm^2$ at SSD = 90 cm.

The clinical patient CT scan was performed during expiratory breath holding in a CT scanner (Lightspeed RT16, GE Healthcare, Little Chalfont, UK). Breath holding was coordinated in the expiratory phase with Abches (APEX Medical,

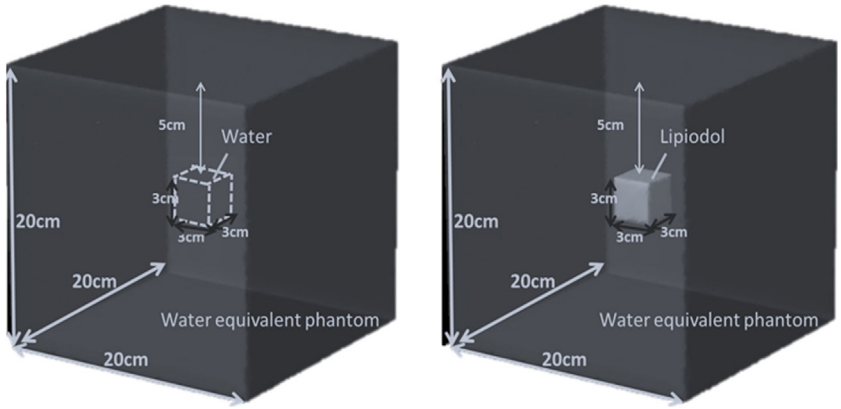


**Fig. 1 – Geometric scheme of virtual phantom without Lipiodol (left) and with Lipiodol (right) located at a depth of 5.0 cm in a water-equivalent phantom (20 × 20 × 20 cm$^3$).**

Tokyo, Japan), which allows patients to control their respiratory motion. The scanned CT image had slice thickness of 1.25 mm and slice interval of 1.25 mm. The CT image, structure, and plan data were exported to our in-house system with MATLAB (The MathWorks, Natick, MA), which operated and translated the data into the format for MC calculations. Then, the patient was represented in a digitized box with the same geometry as the scanned CT image. This box preserves the spatial location of the original CT voxel, Hounsfield unit (HU), and structure data. The material assignment for the Lipiodol was performed with the structure of Lipiodol, which was already contoured in the treatment-planning system Eclipse (Varian Medical Systems, Palo Alto, USA). The materials without Lipiodol were assigned with the conversion of the CT value to the materials using the same method as the Acuros XB (AXB) algorithm in Eclipse. The tumor volume enhanced by residual Lipiodol and the dynamic CT in treatment planning CT were defined as the Gross Tumor Volume (GTV). The margin of the Clinical Target Volume (CTV) and a Planning Target Volume (PTV) were added, typically 5 mm around the GTV and 5–8 mm, which includes the respiratory motion reproducibility and setup error. The clinical plan with eight beams (four coplanar and four non-coplanar beams) was used.

### 3.2. *Lineal energy distribution*

PHITS used a mathematical function that expresses the microdosimetric probability densities (PDs) as a function of LET of ionizing particles, energy and the charge to calculate the PDs in a macroscopic matter within a reasonable computational time. The lineal energy (y) distribution is the quotient of the energy deposited into a volume of interest. The y distribution is deposited by ionizing radiation in the microscopic sites that causes lethal lesions of DNA.[21] The y distribution with 6-MV x-ray beam was calculated using the T-SED function of PHITS.[22] For the y distribution, the simulation model was created with a track structure simulation. The domain size was assumed to be composed of spherical sites with diameters from 1 nm to 1 μm. An analytical function was developed based on this result. Thus, the domain size in the current study was 0.5 μm for the calculation of lineal energy distribution. Subsequently,

**Table 1 – Radiobiological characteristics of HepG2 described with parameters derived from the dose-survival curves fitted with a standard LQ model and incomplete repair model referenced by Zheng et al.[23]**

| Parameters | Values |
|---|---|
| $\alpha$(Gy$^{-1}$) | 0.118 |
| $\beta$ (Gy$^{-2}$) | 0.038 |
| $\alpha/\beta$ (Gy) | 3.1 |
| $T_{1/2}$ (min) | 22 |

the dose-mean linear energy $y_D$ was calculated using the linear energy y as follows:

$$y_D = \frac{\int y^2 f(y)\,dy}{\int y f(y)\,dy} = \frac{\int y d(y)\,dy}{\int d(y)\,dy} \quad (1)$$

where $f(y)$ is the PD of the lineal energy and $d(y)$ is the dose distribution of the lineal energy.

### 3.3. *Survival fraction with physical dose and cell parameters*

The $\alpha_0$ is the proportionally factor to $D$ [Gy$^{-1}$] and $\beta_0$ is the proportionality factor to $D^2$ [Gy$^{-2}$] which are obtained by the survival fraction in the LQ model. Table 1 shows the cell parameters of the HSG tumor cells and the calculated $y_D$ values for the 6-MV x-ray beam, which was the dose-mean lineal energy, referenced from a previous study.[23] According to their transformations, the relation between the dose and cell SF can be deduced by solving the rate equations for the number of potentially lethal lesions (PLLs) and lethal lesions (LLs) are classified into four categories: (1) irreparable lethal lesion (LL) that emergesemerge at constant rate $a$ through first-order process; (2) converted to LLs through second-order process; (3) repaired at constant rate $c$ through first-order process; (4) persisting for a length of time $t_r$, after which it becomes lethal and unrepairable. The constants $a$ and $c$ were derived in a previous study.[11] Moreover, this previous study assumed that the PLL

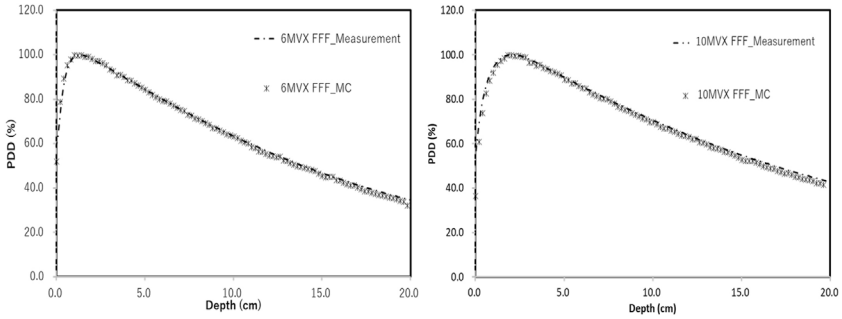


**Fig. 2 – Validation of MC-calculated PDD curves compared with the measurement with the chamber for FFF beam of 6MVX (left) and 10MVX (right).**

repair rate, which was defined as $(a+c)$, was obtained by the DNA repair half-time $T_{1/2}$ of HepG2.[23]

$$a + c = \frac{\ln 2}{T_{1/2}}. \tag{2}$$

The SF in the MK model can be calculated as[17]

$$SF = e^{-\left(\alpha_0 + \frac{y_D}{\rho \pi r_d^2} F\beta_0\right) D_{phys} - F\beta_0 D_{phys}^2} \tag{3}$$

where, F is the Lea–Catcheside time-factor, which is given by[24]

$$F = \frac{2}{(a+c)^2 T^2}\left[(a+c)\,T + e^{-(a+c)T} - 1\right] \tag{4}$$

where T is the total treatment time. The T is calculated by dividing the $D_{phys}$ by the dose rate (DR) that is 0.1–24 Gy/min in this study.

### 3.4. *Biological dose calculation with MC*

The $D_{bio}$ was calculated using the following equation from the study of Inaniwa et al.[17]

$$D_{bio} = \frac{-\alpha_0 + \sqrt{\alpha_0^2 - 4 ln SF D_{phys}\beta}}{2\beta} \tag{5}$$

where the $D_{phys}$ was calculated for the 6MVX and 10MVX FFF beams. $D_{bio}$ depends on the SF, which is the negative of the natural log of the survival fraction at the 10% survival level. The $D_{bio}$ is calculated with the dose rate (DR) between 0.1 and 24 Gy/min.

## 4. Results

### 4.1. *The validation of MC*

Fig. 2 shows the comparison of the measurement and the MC-calculation in the water phantom for 6MVX and 10MVX FFF beams. The step size of the chamber measurements was 2 mm. The calculated dose beyond the build-up point agreed with the measurement within 1.0%.

Fig. 3 shows the physical dose-enhancement factor ($D_{phys}$EF) and biological dose enhancement factor ($D_{bio}$EF). All the PDDs of the physical and biological doses were normalized to 100% at $d_{max}$ for each beam. DEF represents the ratio of the deviation of $D_{phys}$ deposited with Lipiodol and the $D_{phys}$ deposited without Lipiodol divided by the $D_{phys}$ deposited without Lipiodol. $D_{bio}$ EF represents the ratio of the deviation of the $D_{bio}$ deposited with Lipiodol and the $D_{bio}$ dose deposited without Lipiodol divided by the $D_{bio}$ dose deposited without Lipiodol. In Fig. 3, $D_{bio}$ was calculated using DR = 2 Gy/min. The $D_{phys}$EF and $D_{bio}$EF at the center of the Lipiodol region (depth 6.5 cm) were 17.0% and 20.8% for the 6MVX FFF beam, and 10.5% and 11.4% for the 10MVX FFF beam, respectively. The average difference between $D_{phys}$EF and $D_{bio}$EF was 3.8% and 1.0% for 6MVX and 10MVX FFF beams, respectively.

Fig. 4 shows the $D_{bio}$EF calculated with DR = 0.1–24 Gy/min. There was a small difference within 1% between the $D_{bio}$EF values with DR = 0.5–24 Gy/min for both 6MVX FFF and 10MVX

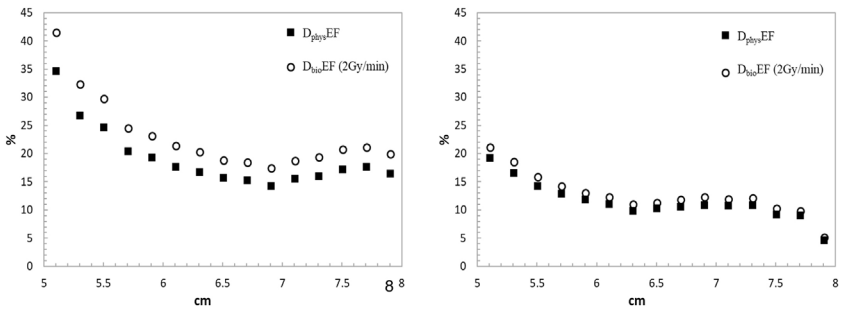


**Fig. 3 – The $D_{phys}$ (closed squares) and $D_{bio}$ (open circles) with DR = 2 Gy/min at 5–8 cm for 6MVX (left) and 10MVX FFF (right) beams.**

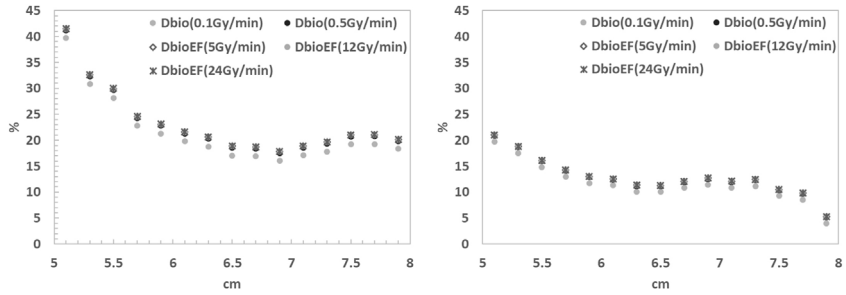


**Fig. 4 – The $D_{phys}EF$ (closed squares) and $D_{bio}EF$ (open circles) with DR = 0.1–24 Gy/min at 5–8 cm for 6MVX FFF (left) and 10MVX FFF (right) beams.**

FFF beams. On the other hand, the average difference between DR = 0.1 Gy/min and 0.5–24 Gy/min was 1.8% for 6MVX FFF and 1.3% for 10MVX FFF beams, respectively. This difference was larger for the 6MVX FFF beam than for the 10MVX FFF beam.

Fig. 5 shows the physical and biological dose distributions with 2 Gy/min in the axial plane for a clinical case of liver SBRT. The dose distributions were normalized by the prescription dose. The red region indicates dose greater than 90% in the figure. This region volume is larger in the physical dose distribution with Lipiodol than that without Lipiodol. Comparing the physical dose distribution with the biological dose distribution with 2 Gy/min, the red washed region indicates that dose greater than 90% was larger for the $D_{bio}$ with 2 Gy/min.

Fig. 6 shows the lateral dose profile of the physical and biological dose distributions with and without Lipiodol in the isocenter plane. The average $D_{phys}EF$ and $D_{bio}EF$ in GTV were 6.0% and 8.1%. The $D_{bio}EF$ was larger than $D_{phys}EF$ in the Lipiodol-uptake region.

## 5. Discussion

Our previous study reported the $D_{phys}EF$ in the Lipiodol region for a 10MVX FFF beam. The $D_{bio}EF$ with 2 Gy/min was larger than $D_{phys}EF$ for both 6MVX and 10MVX FFF beams. The relation between the RBE and DEF is not nonlinear, and RBE may depend not only on the total energy deposited but also the spatial pattern of radiation-induced ionizations.[25–27] The previous study reported SF and RBE data showing dose enhancement with AuNPs.[28] Herold et al. reported the RBE and tumor-control probability (TCP) enhancement with the high-Z material.[29] However, the RBE indicated the biological effects, but the dose evaluation considering the biological effects should be used in clinical applications. In the current study, the $D_{bio}EF$ was calculated by varying the dose rate derived from MK model. The $D_{bio}EF$ was larger than $D_{phys}EF$, which could indicate that the tumor region containing the Lipiodol is expected to increase the local control biologically. Further study of the TCP calculation is needed.

Lohse et al. showed that clonogenic survival is statistically reduced if the total dose is delivered with a higher dose per pulse.[30–32] Thus, the high-dose-rate beam might reduce cell survival by an increase in DNA damage induction, especially an increase in double-strand breaks (DSB) that arise after irradiation because of their impact on genome stability and cell survival. From the results of the current study, the difference in the $D_{bio}EF$ was very small, within 1.0% at 0.2–24 Gy/min for both the 6MVX and 10MVX FFF beams. On the other hand, the difference of the DbioEF at 0.1 Gy/min and 0.2–24 Gy/min was over 1.0% for both the 6MVX and 10MVX FFF beams. Therefore, a higher biological dose enhancement is expected through the use of a high dose rate of more than 0.2 Gy/min.

Herold et al. reported that an increased biologically effective dose could be produced by gold microspheres suspended in cell culture or distributed in tumor tissue exposed to kilovoltage photon beams.[28] Ferrero et al. also reported that the

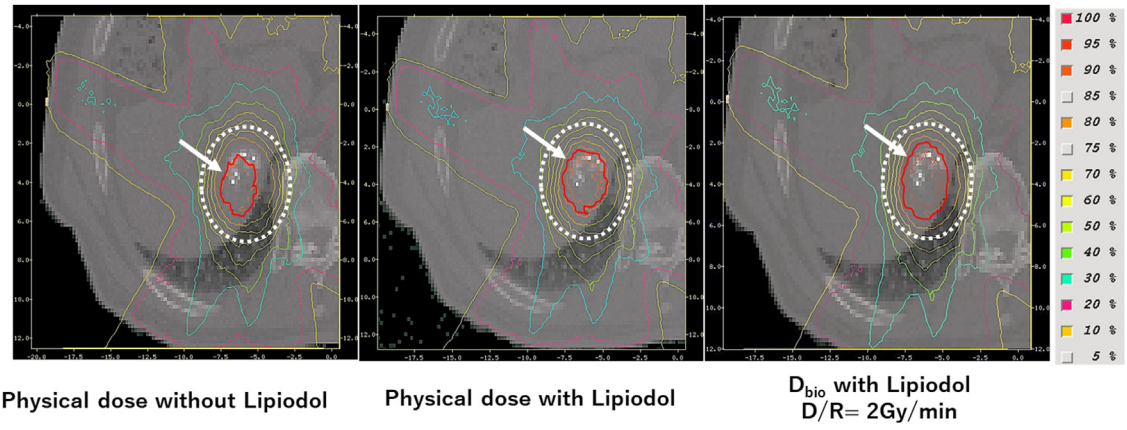


**Fig. 5 – The physical dose distribution without Lipiodol (left), with Lipiodol (center), and biological dose distribution at DR = 2 Gy/min (right) for 10MVX FFF beam using clinical patient CT.**

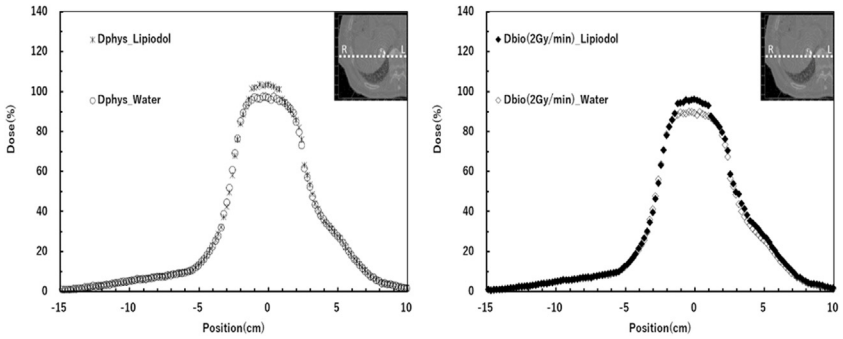


**Fig. 6 – Comparison of the physical dose profile (left) and biological dose profile with 2 Gy/min (right) with and without Lipiodol for 10MVX FFF beams.**

model suggests an RBE and TCP enhancement when lower energies are used in the presence of GNPs.[33] For the difference between the 6MVX and 10MVX beams, the same trend was found as the difference between $D_{bio}EF$ and $D_{phys}EF$ from the comparison of the 6MVX FFF beam that included lower photon energies and the 10MVX FFF beam that included higher photon energies.

However, there were two limitations to the current study. One was that biological experimental data with Lipiodol cannot be obtained. However, Zygmanski et al. reported that predictions of a theoretical SF are possible by employing a model of X-ray-induced damage in the dose-enhancement regions.[34] Therefore, it is possible to calculate the biological dose in the presence of Lipiodol from the theoretical SF and physical dose. The other was the arrangement of Lipiodol molecules and tumor cells. The molecule-size-based calculation was not performed in the current study. Lechtman et al. reported that the photon source energy and the size of the high-Z material influence the spatial distribution of the energy deposited around the high-Z material.[35] Thus, electrons lose their energy over a larger distance and can cross-fire between cells, but they can still cause significant DNA damage. The future work of this study is focused on considering the microscopic spatial relationship between Lipiodol and cells.

## 6. Conclusions

The current study evaluated the biological dose enhancement for Lipiodol. The lower-energy and higher-dose-rate beams were contributed to the biological dose. The Lipiodol caused the enhancement of the physical dose and biological effectiveness.

## Conflict of interest

None declared.

## Financial disclosure

None declared.

## REFERENCES

1. Hainfeld J, Slatkin D, Smilowitz H. The use of gold nanoparticles to enhance radiotherapy in mice. *Phys Med Biol* 2004;**49**:309–15.
2. Matsudaira H, Ueno AM, Furuno I. Iodine contrast medium sensitizes cultured mammalian cells to X rays but not to gamma rays. *Radiat Res* 1980;**84**(1):144–8. PubMed PMID: 7454977.
3. Jain S, Hirst DG, O'Sullivan JM. Gold nanoparticles as novel agents for cancer therapy. *Br J Radiol* 2012;**85**:101–13.
4. Chithrani DB, Jelveh S, Jalali F, et al. Gold nanoparticles as radiation sensitizers in cancer therapy. *Radiat Res* 2010;**173**:719–28.
5. Leung MKK, Chow JC, Lee MJ, Oms B, Jaffray DA. Irradiation of gold nanoparticles by x-rays: Monte Carlo simulation of dose enhancements and the spatial properties of the secondary electrons production. *Med Phys* 2011;**38**:624–31.
6. Lechtman E, Chattopadhyay N, Cai Z, Mashouf S, Reilly R, Pignol JP. Implications on clinical scenario of gold nanoparticle radiosensitization in regards to photon energy, nanoparticle size, concentration and location. *Phys Med Biol* 2011;**56**:4631–47.
7. McMahon SJ, Hyland WB, Muir MF, et al. Biological consequences of nanoscale energy deposition near irradiated heavy atom nanoparticles. *Sci Rep* 2011;**1**:18.
8. Jones BL, Krishnan S, Cho SH. Estimation of microscopic dose enhancement factor around gold nanoparticles by Monte Carlo calculations. *Med Phys* 2010;**37**(Jul (7)): 3809–16.
9. Kawahara D, Ozawa S, Saito A, et al. Dosimetric Impact of Lipiodol in Stereotactic Body Radiation Therapy on Liver after Trans-arterial Chemoembolization. *Med Phys* 2017;**44**(Jan(1)):342–8.
10. Kawahara D, Ozawa S, Saito A, et al. Energy spectrum and dose enhancement due to the depth of the Lipiodol position using flattened and unflattened beams. *Rep Pract Oncol Radiother* 2018;**23**(Jan-Feb (1)):50–6.
11. Joiner M, van der Kogel AJ. The dose-rate effect. In: Joiner M, van der Kogel AJ, editors. *Basic Clinical Radiobiology*. London: Edward Arnold; 2009. p. 158–68.
12. Guan F, Bronk L, Titt U, et al. Spatial mapping of the biologic effectiveness of scanned particle beams: towards biologically optimized particle therapy. *Sci Rep* 2015;**18**(5):9850.
13. Bauchinger M, Schmid E, Streng S, Dresp J. Quantitative analysis of the chromosome damage at first division of human lymphocytes after 60Co-γ -irradiation Radiat. *Environ Biophys* 1983;**22**:225–9.

14. Kawahara D, Nakano H, Ozawa S, et al. Relative biological effectiveness study of Lipiodol based on microdosimetric-kinetic model. *Phys Med* 2018;**46**:89–95.
15. Okamoto H, Kanai T, Kase Y. Relation between lineal energy distribution and relative biological effectiveness for photon beams according to the microdosimetric kinetic model. *J Radiat Res* 2011;**52**(1):75–81.
16. Hawkins RB. A microdosimetric-kinetic model of cell death from exposure to ionizing radiation of any LET, with experimental and clinical applications. *Int J Radiat Biol* 1996;**69**:739–55.
17. Inaniwa T, Suzuki M, Furukawa T, et al. Effects of dose-delivery time structure on biological effectiveness for therapeutic carbon-ion beams evaluated with microdosimetric kinetic model. *Radiat Res* 2013;**180**(Jul (1)):44–59.
18. Elkind MM, Sutton H. Radiation response of mammalian cells grown in culture. Repair of X-ray damage in surviving Chinese hamster cells. *Radiat Res* 1960;**13**:556–93.
19. Kawrakow I, Mainegra-Hing E, Rogers DWO, Tessier F, Walters BRB. *The EGSnrc code system: Monte Carlo simulation of electron and photon transport*. Ottawa, Canada: NRCC: National Research Council of Canada Report PIRS-701; 2013.
20. Puchalska M, Sihver L. PHITS simulations of absorbed dose out-of-field and neutron energy spectra for ELEKTA SL25 medical linear accelerator. *Phys Med Biol* 2015;**60**:261–70.
21. ICRU. *Microdosimetry ICRU report 36, International Commissioning on Radiation Units and Measurements*. MD: Bethesda; 1983.
22. Sato T, Watanabe R, Niita K. Development of a calculation method for estimating specific energy distribution in complex radiation fields. *Radiat Prot Dosimetry* 2006;**122**(1-4):41–5. Epub 2006 Nov 28.Epub 2006 Nov 28.
23. Zheng Xiao-Kang, Chen Long-Hua, Yan Xiao, et al. Impact of prolonged fraction dose-delivery time modeling intensity-modulated radiation therapy on hepatocellular carcinoma cell killing. *World J Gastroenterol* 2005;**11**(Mar 14 (10)):1452–6.
24. Brenner DJ. The Linear-Quadratic Model Is an Appropriate Methodology for Determining Isoeffective Doses at Large Doses per Fraction. *Semin Radiat Oncol* 2008;**18**:234–9.
25. Zheng Y, Hunting DJ, Ayotte P, et al. Radiosensitization of DNA by gold nanoparticles irradiated with high-energy electrons. *Radiat Res* 2008;**169**:19–27.
26. Xiao F, Zheng Y, Cloutier P, et al. Sanche, On the role of low-energy electrons in the radiosensitization of DNA by gold nanoparticles. *Nanotechnology* 2011;**22**:239–45.
27. Jeong SY, Park SJ, Yoon SM, et al. Systemic delivery and preclinical evaluation of Au nanoparticle containing beta-lapachone for radiosensitization. *J Controlled Dis* 2009;**139**:239–45.
28. Herold DM, Das IJ, Stobbe CC, et al. Gold microspheres: a selective technique for producing biologically effective dose enhancement. *Int J Radiat Biol* 2000;**76**:1357–64.
29. Ferrero V, Visonà G, Dalmasso F, et al. Targeted dose enhancement in radiotherapy for breast cancer using gold nanoparticles, part 1: a radiobiological model study. *Med Phys* 2017;**44**(May (5)):1983–92.
30. Lohse I, Lang S, Hrbacek J, et al. Effect of high dose per pulse flattening filter-free beams on cancer cell survival. *Radiother Oncol* 2011;**101**(Oct (1)):226–32.
31. Steel GG. Cellular sensitivity to low dose-rate irradiation focuses the problem of tumor radioresistance. *Radiother Oncol* 1991;**20**:71–83.
32. Steel GG, Down JD, Peacock JH, Stephens TC. Dose-rate effects and the repair of radiation damage. *Radiother Oncol* 1986;**5**:321–31.
33. Ferrero V, Visonà G, Dalmasso F, et al. Targeted dose enhancement in radiotherapy for breast cancer using gold nanoparticles, part 1: a radiobiological model study. *Med Phys* 2017;**44**(May (5)):1983–92.
34. Zygmanski W Hoegele, Tsiamas P, et al. A stochastic model of cell survival for high-Z nanoparticle radiotherapy. *Med Phys* 2013;**40**(Feb (2)):024102.
35. Lechtman E, Chattopadhyay N, Cai Z, Mashouf S, Reilly R, Pignol JP. Implications on clinical scenario of gold nanoparticle radiosensitization in regards to photon energy, nanoparticle size, concentration and location. *Phys Med Biol* 2011;**56**(15):4631–47.